View metadata, citation and similar papers at core.ac.uk
brought to you by CORE
provided by Digital.CSIC

Environmental forcing and the larval fish community associated to the Atlantic bluefin tuna spawning habitat of the Balearic region (Western Mediterranean), in early summer 2005

J.M. Rodriguez*, I. Alvarez[1], J.L. Lopez-Jurado[2], A. Garcia[3], R. Balbín[2], D. Alvarez-Berasategui[4], F.Alemany[2]

Instituto Español de Oceanografía, Centro Oceanográfico de Gijón, Avda. Príncipe de Asturias 70Bis, 33212 Gijón, Asturias, Spain
[1]IMEDEA-CSIC, Miquel Marqués, 21, 07190 Esporles, Baleares, Spain
[2]Instituto Español de Oceanografía, Centro Oceanográfico de Baleares, Muelle de Poniente s/n, Apdo. 291, 07015 Palma de Mallorca, Spain.
[3]Instituto Español de Oceanografía, Centro Oceanográfico de Málaga, Aptdo. 285, 29640 Fuengirola, Málaga, Spain
[4]SOCIB, Balearic Islands Coastal Observing and Forecasting System, Palma deMallorca, Spain

*Corresponding author. Tel: +3485308672; Fax: +3485326277.
E-mail address: j.m.rodriguez@gi.ieo.es (J.M. Rodriguez).

Abstract

The Balearic region is a highly dynamic area located in the Western Mediterranean, straddling the transition between the Algerian and Provencal basins and constitutes one of the main spawning grounds for the large, migratory Atlantic bluefin (*Thunnus thynnus*) and other medium and small tuna species (*Thunnus alalunga, Auxis rochei, Euthynnus alleteratus* and *Katsuwonus pelamis*). In summer, despite been considered an oligotrophic region as the whole Mediterranean Sea, it harbors a relatively abundant and diverse larval fish community (LFC). In this study, we analyze the composition, abundance and the influence of abiotic and biotic factors on the horizontal structure of the LFC in the Balearic region, in early summer 2005, during the spawning season of Atlantic bluefin tuna. Hydrographically, 2005 was an unusual year with a summer situation of relatively lack of mesoscale features, weak surface currents and a general situation of high stability. A total of 128 taxa of fish larvae, belonging to 52 families, were identified. The average abundance was 1770 larvae 1000 m^{-3}. Multivariate statistical analysis revealed LFC to have a strong horizontal structure. Cluster analysis

and non-metric multidimensional scaling ordination identified two larval fish assemblages. These assemblages were mainly delineated by depth and, therefore, by the spawning location of adult fish. Our results also suggest that anticyclonic eddy boundaries constitute favourable habitats for fish larvae. Also, the scenario of higher than unusual hydrographic stability found during the cruise would be responsible for the relatively lack of mesoscale features and, consequently, for the lack of influence of these features on the horizontal distribution of fish larvae and on the horizontal structure of the LFC.

Key words: Western Mediterranean, Balearic region, Hydrography, Ichthyoplankton, Larval fish community, Tuna spawning habitat

Introduction

The Balearic region is a highly dynamic area located in the Western Mediterranean (Fig. 1). The Balearic Archipelago straddles the transition between the Algerian and Provencal basins and plays a key role in the water mass dynamics in the Central Western Mediterranean, by conditioning water mass exchange between the two basins, through the island channels (Lopez-Jurado *et al.*, 1995; Pinot *et al.*, 2002). The input flow of Atlantic Water (AW), through the Gibraltar strait, cross the Alboran Sea and enters the Algerian basin following the North African coast, forming the Algerian Current (AC). A thermohaline front, the Almeria-Oran front (Fig. 1), is formed by the convergence of surface Atlantic waters, less saline, and Mediterranean surface waters, more saline (Tintore *et al.*, 1991). The unstable character of the AC sometimes leads to the generation of cyclonic and anticyclonic eddies (Millot, 1985, 1999). Anticyclonic eddies have a lifetime of weeks to months, move freely within the Algerian Basin and

some of them reach the Balearic Islands (Font *et al.*, 2004; Millot, 1987). Filaments of AW, generated when the thermohaline Almeria-Oran front becomes unstable (Tintore *et al.*, 1988), can also reach and even surpass the Balearic archipelago through the island channels (Fig. 1). In the Provencal basin, the Northern Current (NC) flows southwestward, along the continental slope (Fig. 1). A branch of the NC forms the Balearic Current (BC) that flows northeastward, along the northern slope of the Balearic Islands (Fig. 1). A surface front, the Balearic Front, associated with the BC, and continued in the east by the North Balearic Front (Fig. 1), separates fresher AW of the Algerian basin from colder and saltier resident AW of the Provencal basin (Salat, 1995). The surface circulation is mainly driven by density in the Algerian basin while in the Provencal basin is mainly driven by atmospheric forcing, largely wind (Hopkins, 1978). As consequence, hydrodynamic conditions in the north and south of the islands are quite different (Lopez-Jurado *et al.*, 2008).

The Balearic region, as the whole Mediterranean Sea, is considered an oligotrophic region during the summer stratification period (Estrada, 1996; Fernández de Puelles *et al.*, 2007). During summer, in the absence of riverine nutrient input (it must be pointed out that there are no permanent freshwater streams in the Balearic Islands), the biological production is mainly associated with mesoscale oceanographic features, fronts and eddies (Alcaraz *et al.*, 2007; Estrada *et al.*, 1993; Jansa *et al.*, 2004; Jansa *et al.*, 1998). Also, the vertical distribution of chlorophyll shows a deep chlorophyll maximum (DCM), typical of oligotrophic regions, located below the thermocline (Estrada *et al.*, 1993; Jansa *et al.*, 1998). The maximum concentration of zooplankton coincides with the DCM, where zooplankton is feeding (Alcaraz *et al.*, 2007; Saiz *et al.*, 2007).

Despite its oligotrophy, the Balearic region harbors a relatively diverse and abundant summer larval fish community (LFC) (Alemany, 1997; Alemany *et al.*, 2006; Sabates *et al.*, 2007). In addition, this region is recognized as one of the main spawning areas for the eastern Atlantic stock of the large migratory Atlantic bluefin (*Thunnus thynnus*), other medium and small tuna species (*Thunnus alalunga*, *Auxis rochei*, *Euthynnus alleteratus, Katsuwonus pelamis*) and other large pelagics, such as, *Xiphias gladius* or *Coryphaena hippurus* (Alemany *et al.*, 2010). The presence of larvae of these species, the reproductive strategy of most of fish species in the northwestern Mediterranean, which reproduce in spring-summer (Olivar *et al.*, 2010; Sabates *et al.*, 2007), and the mesoscale oceanographic features, enhancing biological productivity, may account for the relatively high species richness and larval fish abundances recorded in the area. On the other hand, processes such as currents, fronts and eddies influence the distribution, abundance and survival of fish larvae and, accordingly, define the abundance, structure and diversity of the LFC (Bakun, 2006; Holliday *et al.*, 2011; Lobel and Robinson, 1988; Mullaney *et al.*, 2011; Rodriguez *et al.*, 2004; Sabates and Olivar, 1996).

The summer LFC of the Balearic region has been previously studied but at a short spatial scale. In this study, the most geographically widespread carried out on the ichthyoplankton in the region, we analyse the composition, abundance and the horizontal structure of the LFC of the Balearic region, in early summer 2005. We also analyse the influence that abiotic (depth, sea surface salinity, dynamic height and geostrophic velocity and biotic environmental factors (phytoplankton and mesozooplankton biomass) have on the horizontal structure of the LFC. We hypothesized that the horizontal distribution of fish larvae and, consequently, the horizontal structure of the LFC would reflect the mesoscale oceanographic features of the region.

Material and methods

Data collection

This study is based on data collected during the Tunibal 05 oceanographic-ichthyoplankton survey, carried out in the Balearic region (NW Mediterranean), in summer (from June 27 to July 23) 2005 (Fig. 1). A total of 190 (183 for ichthyoplankton) stations, arranged in a regular sampling grid of 10 x 10 nm, were sampled.

At every station, vertical profiles of conductivity, temperature and fluorescence were obtained with a Sbe 911 CTD. Profiles were to 350 m in depth (160 stations), or to 650 m at selected stations (30 stations).

Zooplankton samples were collected with a Calvet net equipped with 55 µm mesh nets in vertical hauls, from 70 m depth to the surface. Samples were filtered immediately through 200 µ and 2 mm mesh filters to separate the three zooplankton fractions. The macrozooplankton fraction was discarded and both, the micro and mesozooplancton samples where then placed in Petri dishes and frozen at -20 ºC. In the laboratory, the micro and mesozooplankton dry weight were obtained following (Lovegrove, 1966). Nonetheless, microzoplankton was not considered because for many samples their dry weight was below the detection limit of the precision balance used. Mesozooplankton dry weight biomass values were standardised to mg m^{-3}.

Ichthyoplankton samples were collected with a Bongo 60 net equipped with 200 and 335 µm mesh nets. Tows were oblique trying to reach 70 m depth, apart from three stations shallower than 70 m. At every station, the length of the wire was adjusted in function of the wire angle to reach 70 m depth. The volume of water filtered was measured by two flowmeters (General Oceanics) installed in the mouths of each net.

135 Ichthyoplankton samples were immediately preserved in a 4% sodium-borate buffered
136 solution of seawater and formaldehyde. In the laboratory, all fish larvae were sorted
137 from the 335 µm mesh net samples, counted and identified to the lowest taxonomic
138 level possible. Larval fish catches at each station were standardised to number 1000 m^{-3}.

139

140 Data analysis

141 Temperature, salinity and fluorescence records at each station were processed at their
142 original sampling frequency and averaged at 1 m interval. Horizontal hydrographic
143 fields were obtained with a standard optimal interpolation scheme, using an isotropic
144 Gaussian correlation (Bretherton *et al.*, 1976; Pedder, 1993). The dynamic height at 10
145 dbar was calculated by vertical integration of the specific volume anomaly from the
146 level of 600 dbar, which was chosen as the level of no motion (Pinot *et al.*, 2002). At
147 shallow stations, or when data were recorded only down to 350 m, the density anomaly
148 at the closer 600 m station was assigned to the deepest level sampled by the CTD.
149 Geostrophic velocities were obtained using the first-derivative of the dynamic height
150 fields (Pinot et al., 2004). Dynamic height was used as an indicator of eddies and frontal
151 regions, because dynamic height should be higher than average in anticyclonic and
152 frontal regions and lower than average in cyclonic eddy regions (Lindo-Atichati *et al.*,
153 2012 and references therein). Geostrophic velocity at 10 m depth was used as an
154 indicator of eddy boundaries and frontal regions, because geostrophic velocity should
155 be higher in these regions (Bakun, 2006; Le Febre, 1986; Sournia, 1994).

156 In early summer, the surface warming in the Mediterranean Sea is strong. Thus, sea
157 surface temperature (SST) does not depend on the geographical position but on
158 sampling date. As consequence, temperature was not useful for characterizing surface

159 water masses. Sea surface salinity (SSS), salinity at 10 m depth, was considered the best
160 parameter for this purpose.

161 The relation between environmental variables, SSS, dynamic height, geostrophic
162 velocity, depth-integrated (5-200 m) fluorescence, as an estimate of phytoplankton
163 biomass, mesozooplankton biomass and larval fish concentration was tested using
164 Pearson's correlation coefficient in SPSS v. 19.0.

165 Taxon diversity was calculated for each station using the Shannon-Wiener diversity
166 index (*H'*) in PRIMER v. 6.1.6 (Plymouth Routines In Multivariate Ecological
167 Research).

168 Following Clarke and Ainsworth (1993) and Field *et al.* (1982), non-parametric
169 multivariate techniques in PRIMER were used to study the horizontal structure of the
170 LFC. Cluster analysis in conjunction with non-metric multidimensional (MDS)
171 ordination was used to identify larval fish and taxa assemblages. Only "non rare taxa,
172 those found in >5% of the stations and/or had a relative abundance of >0.04%, were
173 included in the analysis. Cluster analysis and MDS were performed on a Bray-Curtis
174 similarity matrix (Bray and Curtis, 1957), generated from the $\log_e$ (x+1) transformed
175 data of larval fish abundances. Data were transformed to down-weight the influence of
176 more abundant taxa (Clarke and Ainsworth, 1993; Field *et al.*, 1982). Hierarchical
177 agglomerative clustering with group-average linking, carried out on the similarity
178 matrix, was used to delineate assemblages with distinct community structure. Arbitrary
179 cut-off levels were chosen on dendrograms to produce ecologically interpretable
180 clusters (Field *et al*, 1982; Auth and Brodeur, 2006). The adequacy of the classification
181 analysis was checked by superimposing the results of the clustering on MDS plots
182 generated from the same similarity matrices (Auth and Brodeur, 2006; Clarke and
183 Ainsworth, 1993; Clarke and Warwick, 2001). A 2-dimensional ordination approach

184 was adopted because the stress level (≤0.16) was acceptably low (Clarke and
185 Ainsworth, 1993; Clarke and Warwick, 2001).

186 The relationship between biological and environmental variables and "non rare" taxa
187 was assessed with Canonical Correspondence Analysis (CCA) in CANOCO 4.5 (ter
188 Braak and Smilauer, 2002). CCA is a multivariate method to elucidate the relationships
189 between assemblages of species and their environment (ter Braak and Verdonschot,
190 1995). Rare species, as above, were not included in the analysis. Larval abundances
191 were $\log_e (x+1)$ transformed before analysis. The explanatory variables were station
192 depth, SSS, dynamic height, geostrophic velocity, depth-integrated fluorescence and
193 zooplankton biomass. SST was not included in the analysis because of is temporal
194 variability, daily increase, as indicated above. Canonical axes were tested for
195 significance with a Monte Carlo permutation test (9999 permutations) in CANOCO (ter
196 Braak and Smilauer, 2002).

197

198 **Results**

199 Hydrography and plankton

200 In summer, in the absence of the winter atmospheric forcing, the density gradient
201 dominates and allows AW inputs to enter the Balearic region. Thus, the southernmost
202 part of our study area was occupied by fresh AW (salinity <37.5) (Fig. 2a). Weak inputs
203 of this water crossed the Ibiza channel and, surrounding the northern Ibiza Island,
204 returned into the Algerian basin through the Mallorca channel. The northeastern corner
205 was occupied by resident AW (salinity >38), isolated patches of resident AW were also
206 found in the north of the area, and the rest of the region was occupied by mixed AW
207 (salinity 37.5 ─ 38) (Fig. 2a). Consequently, the boundary between fresh and resident

AW was found south of the archipelago. The main hydrographic mesoscale features observed during the study were two anticyclonic eddies. A strong, fresh AW anticyclonic eddy was located south of the Mallorca Channel, centered at 38.5^{o} N (Fig. 2b). Another weak, mixed AW anticyclonic eddy was found at the east of Mallorca and the south of Menorca Island (Fig. 2b). Surface currents, including the BC flow, were also relatively weak (Fig. 2b).

The water column showed a strong thermal stratification. The mixed layer, defined as the layer where temperature and salinity were homogeneous due to solar heating and turbulence induced by weak easterlies, was 15 m of average thickness and with temperatures between 20 and 26 ºC. It was followed by a strong thermal gradient to around 60 m depth. From this depth to 150 m, the temperature decreased gradually to reach ~13 ºC, the deep-water temperature (Fig. 3). As mentioned above, SST depended on sampling date. Thus, the lowest SST was recorded at the beginning of the cruise and the highest SST was measured at the end of the cruise. In fact there was a significant correlation between SST and sampling dates ($r = 0.62$ for temperature at 5 m depth and $r = 0.34$ for temperature at 10 m depth, $p < 0.01$ in both cases).

The vertical distribution of fluorescence showed a deep fluorescence maximum (DFM) located at an average depth of about 75 m, below the thermocline (Fig. 3). The horizontal distributions of depth-integrated fluorescence and mesozooplankton biomass showed irregular patterns (Fig. 4). The most noticeable feature of these distributions was that the highest values for both these biological variables were recorded in the oceanic region. In fact, the correlation of depth-integrated fluorescence and mesozooplankton biomass with depth was significant ($r = 0.30$, $p < 0.01$ and $r = 0.16$, $p < 0.05$, respectively). Also, it must be pointed out that the correlation between them was not significant.

The larval fish community

A total of 54545 fish larvae were caught in this study, including 128 taxa belonging to 52 families (Table I). Myctophydae, with 17, and Gobiidae, with 12, were the families with the largest number of taxa. The abundance of fish larvae ranged from 90 to 5991 L 1000 m^{-3}, with a mean of 1770 L 1000 m^{-3}. Larvae of the families Myctophidae, which accounted for 50% of total catch, and Gonostomatidae, 33% of total catch, were the most abundant. *Hygophum* spp was the most abundant and one of the most common taxa, accounting for 25.1% of the total larval fish abundance and being caught at 95.1% of the stations. The second most abundant species was *Cyclothone braueri* (24.6%), which also was the most common taxa, appearing at almost all stations (98.9%). Other abundant and common taxa were *Ceratoscopelus maderensis*, 14.3% of the larval fish abundance and appearing at 97.8% of the stations, *Cyclothone pygmaea*, 7.6% of the larval fish abundance and captured at 91.8% of the stations and *Lampanyctus crocodilus* that accounted for 4.2% of the larval fish abundance and was captured at 89.1% of the stations. Only for three neritic species their relative abundances were above 1% of total larval catch. These species were *Auxis rochei*, which accounted for 2.3% of larval fish abundance and was caught at 44.8% of the stations, *Sardinella aurita*, 1.6% of the larval abundance and caught in 25.7% of the stations and *Engraulis encrasicolus*, 1.4% of the larval fish abundance and present in 33.9% of the stations. The horizontal distribution of fish larvae, with low concentrations around the islands and the highest recorded away from these (Fig. 5), showed similar pattern to that of depth-integrated fluorescence and mesozooplankton biomass (Fig. 4). Individual species also showed irregular patterns of horizontal distribution (Fig. 5). As expected, larvae of oceanic species showed higher concentrations in the oceanic region and larvae of neritic species showed higher concentration in the neritic region (Fig. 5). Nevertheless, larvae of oceanic species were

caught in the neritic region, as were larvae of neritic species caught in the oceanic region (Fig. 5). Larval fish abundance was correlated with geostrophic velocity ($r = 0.16$, $p < 0.05$) and with the species diversity index ($r = -0.28$, $p < 0.01$).

The number of taxa per station ranged from 7 to 35, with the maximum values recorded around the islands (Fig. 6a). Larval diversity was relatively high, ranging from 0.92 to 2.98. Its horizontal distribution followed a similar pattern to the number of taxa, with the highest values also recorded around the islands (Fig. 6b). Larval diversity was correlated with SSS ($r = 0.34$, $p < 0.01$) and with larval abundance, as indicated above.

Cluster analysis identified two LFAs at a similarity level of 41% (Fig. 7a). MDS ordination produced the same results (Fig. 7b). Assemblages were named after the location of the stations they occupied. The neritic assemblage occupied almost exclusively stations located inside the 200 m isobath, while the oceanic assemblage occupied the stations located outside the 200 m isobath (Fig. 7c). This two group classification was reinforced by the formation by cluster analysis and MDS ordination of two taxa assemblages: a neritic and an oceanic one (Fig. 8). The neritic assemblage was formed by larvae of those taxa that as adults inhabit the neritic region and also reproduce there. The oceanic assemblage was formed by larvae of fish species that as adults live and reproduce in the oceanic region. The allocation of larval fish taxa into one of these two groups was quite accurate, only a taxon *Arnoglossus thori*, a flatfish inhabiting shelf bottoms, clustered with oceanic taxa.

Relationship between larval fish taxa and environment

The Monte Carlo permutation test showed that only the first two canonical axes were significant ($p < 0.05$). These two axes explained 88.0% of the variance of the species–

environment relationship. The species-environment correlation coefficients for the first two CCA axes were 0.70 and 0.56, respectively. In the CCA biplot, environmental variables are represented by arrows, with origin at the centre of the biplot and pointing in the direction of its increase. The length of environmental arrows and their orientation on the biplot determine their relative importance to each axis (ter Braak and Verdonschot, 1995; ter Braak, 1986). Then, according to Figure 9, depth was the most important variable in explaining taxa distribution. This variable, depth-integrated fluorescence, mesozooplankton biomass, dynamic height and geostrophic velocity were negatively correlated with axis 1; only SSS was positively correlated with this axis (Fig. 9). The geographical representation of scores of each station confirms that axis 1 is a depth axis (Fig. 10a). Accordingly, oceanic taxa appeared on the negative side of this axis (Fig. 9). In general, these taxa clustered near the centre of the CCA biplot (Fig. 9). Only two neritic taxa, *Arnoglossus thori* and *Mullus barbatus*, were located on the left side of axis 1, although very close to the right side region of the CCA biplot (Fig. 9). Most taxa that appeared at the very right side of the axis 1 are demersal fish species (e.g. *Gobius niger*, *Spicara smaris*, *Pagrus pagrus* or Ophididae) with relative littoral distribution. Larvae of neritic epipelagic taxa (e.g. *Auxis rochei*, *Trachurus mediterraneus* or *Engraulis encrasicolus*) were located on the right side of Axis I but near of centre of the CCA biplot. Only the oceanic specie *Thunnus thynnus* was located on the right side of the CCA biplot, although near its centre, as most of the oceanic taxa (Fig. 9). Axis 2 was positively correlated with depth and dynamic height (Fig. 9). The geographical representation of scores of each station shows that axis 2, unlike axis 1, could not be identified with any of the environmental variables (Fig. 10). *A. thori*, *Myctophum punctatum*, *Lobianchia dofleini* and *Mullus barbatus* were the species that showed the highest correlation with axis 2 (Fig. 9).

307 The groups of larval fish taxa formed by cluster analysis and MDS ordination (Fig. 8)
308 also appeared in the CCA with little difference (Fig. 9). This indicates strong support of
309 taxa grouping and their relationship with the considered environmental variables (Leps
310 and Smilauer, 2003).

311

312 **Discussion**

313 Hydrography

314 Hydrographically, 2005 was an unusual year because there were consecutive episodes
315 of severe winter leading to violent convective events, with the development of a
316 thermohaline anomaly in deep waters (Lopez-Jurado *et al.*, 2005). Even so, no winter
317 intermediate water (WIW) was formed, since all the surface water masses affected by
318 the cold and intense winter winds became deep Mediterranean waters (Lopez-Jurado *et*
319 *al.*, 2005). In addition, the winter atmospheric forcing, which dominates in the
320 Provencal basin (Hopkins, 1978), favoured that colder and saltier surface waters moved
321 south of the Balearic archipelago (Lopez-Jurado *et al.*, 2005). When this forcing
322 decayed, the recent AW progressed northward generating oceanic fronts along 39º N
323 parallel. During summer, as surface currents were relatively weak, there was no intense
324 inflow of oceanic surface waters towards coastal areas, or currents transporting shelf
325 waters offshore. Also, the Balearic Current Balearic Current (BC) only received weak
326 fresh AW inputs through the Ibiza Channel, because the anticyclonic eddy located south
327 of Mallorca blocked its passage through the Mallorca channel. According to Alemany *et*
328 *al.* (2010), the hydrodynamic scenario observed during this survey was more stable than
329 those found in similar summer surveys carried out in previous years in the region. This

stability would be responsible for the relatively lack of mesoscale hydrographic features found in the area at the time of the study.

During the stratified summer situation and in the absence of riverine nutrient input, the only nutrient source in the region has to be related with the mesoscale oceanographic processes in the region. The horizontal distribution of depth-integrated fluorescence and mesozooplankton biomass, with relatively low concentrations around the islands and the highest values recorded in the oceanic region (Fig. 4), supports that biological production in the region during the study was not related with inputs of nutrients from the islands. It has been reported that Chl a maxima during summer in the Balearic region, are associated with hydrographic features, such as fronts and eddies (Estrada *et al.*, 1993; Jansa *et al.*, 2004; Jansa *et al.*, 1998), which constitute important fertilization sources (Alcaraz *et al.*, 2007; Bakun, 2012). Concretely, during 2001-2003 summers, Jansa et al. (2004) found those maxima, of up to 8 µg l^{-1}, in subsurface strata, in the border of anticyclonic eddies. In this study, the lack of significant correlation of the horizontal distributions of depth-integrated fluorescence with dynamic height and geostrophic velocities did no support the relationship between Chl a and mesoscale hydrographic features. Though, the significant correlation between depth-integrated fluorescence and SSS indicates that biological production was higher in resident AW waters, richer in nutrients than in the fresh, nutrient depleted AW (Estrada, 1996). This relationship of depth-integrated fluorescence with resident AW may mask the relationship of phytoplankton with mesoscale hydrographic features. The most noticeable were the above mentioned two eddies, one of them of fresh and the other of mixed AW (Fig. 2).

The vertical distribution of fluorescence, with a deep fluorescence maximum (DFM), is typical of the Mediterranean Sea during the stratification period (Estrada, 1996). In open

waters off the Balearic Islands, Jansa *et al.* (2004) found significant concentrations of chlorophyll at the DCM level in summer. It has also been reported that during the stratification period, the main zooplankton peak coincides with the DCM (Alcaraz *et al.*, 2007). Copepods nauplii and copepodites, the main food items for fish larvae, also concentrate at this depth (Olivar *et al.*, 2010; Sabates *et al.*, 2009). So, our sampling to 70 m depth, may have not included zooplankton maximum leading to an underestimation of the true values of the mesozooplankton biomass. This also may account for the lack of relationship between the horizontal distribution of depth-integrated fluorescence and mesozooplankton biomass.

The larval fish community

The number of larval fish taxa captured is higher than those found in previous ichthyoplankton studies carried out in our study area, in summer, (Alemany *et al.*, 2006; Torres *et al.*, 2011), off the nearby Catalan coast (Olivar *et al.*, 2010; Sabates, 1990) or in other regions of the Mediterranean Sea, such as the Aegean Sea (Somarakis *et al.*, 2002; Somarakis *et al.*, 2011), Gulf of Gabes (Zarrad et al., 2013) or the Alboran Sea (Rodriguez, 1990). Species richness was only slightly lower or comparable to that reported for subtropical areas (e.g. Keane and Neira, 2008; Moyano and Hernandez-Leon, 2011; Muhling *et al.*, 2008). The higher species richness found in this study in relation with other previously carried out in the region, in summer, may be due to the fact that our study covered a larger area than Alemany *et al.* (2006) and a larger area and sampling deeper than Torres *et al.* (2011). In addition, larvae of large migratory tuna and other pelagic species that reproduce around the Balearic archipelago, the large area covered in this study, including the island shelves and the oceanic region, and the

379 great number of stations sampled could explain the higher specific richness found in this
380 study in relation with other Mediterranean regions.

381 The patterns of horizontal distribution shown by species richness and diversity, with the
382 highest values recorded around the islands, may be related with the narrowness of the
383 island shelves that leads to an overlap of larvae of neritic and oceanic species in the
384 proximity of the islands. Also, eddies found in the area could approach oceanic larvae to
385 the islands, as reported for other marine regions (Franco *et al.*, 2006; Lobel and
386 Robinson, 1986; Olivar *et al.*, 2010). For its part, the negative correlation between
387 larval abundance and species diversity indicates that the increase in larval abundance is
388 related with the proliferation of a single or a few taxa rather than with the increase in
389 abundances of all taxa that made up the larval fish community.

390 Larval fish abundances were also higher than reported for the region by Alemany *et al.*
391 (2006). But, the study of Alemany et al. (2006) was restricted to two small areas off the
392 Mallorca Island, covering the coastal-slope region. So, the fact that larval abundances
393 were higher in the oceanic region would account for the relatively higher larval
394 abundance recorded in this study. Another characteristic of the LFC was that larval
395 abundances were also higher than those found in other more productive marine regions,
396 such as the Taiwan strait (Hsieh *et al.*, 2012) or the California Current region (Auth and
397 Brodeur, 2006). This finding is counterintuitive because the Mediterranean Sea in
398 summer, as mentioned above, is considered oligotrophic. Nevertheless, during this
399 season, in the Western Mediterranean, the DCM and the relatively high zooplankton
400 biomass associated to it (Alcaraz, 1985) offers an important food source for fish larvae
401 (Sabates *et al.*, 2007). Moreover, there may be deep zooplankton hotspots, located in the
402 border of anticyclonic eddies and associated to the phytoplankton hotspots found in
403 other studies (e.g. Jansa *et al.*, 2004). These zooplankton hot spots may also constitute

404 feeding regions for fish larvae. Furthermore, currents that flow through the islands and
405 eddies may trap and transport neritic larvae off the island shelves (Leis, 1982; Lobel and
406 Robinson, 1986; Olivar *et al.*, 2010). In this sense, simulations suggest that during
407 summer a relatively small proportion (~30%) of neritic larvae in the Balearic Islands
408 could be advected offshore (Basterretxea *et al.*, 2012). All these factors may account for
409 the relatively high larval fish abundance found in this study and also for the fact that the
410 higher abundances were recorded in the oceanic region.

411 In addiction, the vertical distribution of larval food would also be favourable for the
412 LFC found in the region. In stratified waters, fish larvae show a stratified vertical
413 distribution. With some exceptions, larvae of neritic species are distributed in the mixed
414 layer and the upper region of the thermocline, while larvae of oceanic species show a
415 deeper distribution, generally below the thermocline (Ahlstrom, 1959). Larvae of neritic
416 taxa caught in this study, apart from e.g. Gobiidae and Callionymidae, show a shallow
417 vertical distribution in the region (Olivar *et al.*, 2010; Olivar and Sabates, 1997; Torres
418 *et al.*, 2011), but also some of them perform daily vertical migrations. This is the case of
419 larger *S. aurita* and *E. encrasicolus* larvae, the second and third most abundant neritic
420 species caught in this study, that move downward during the daytime, to the DCM in
421 the case of *E. encrasicolus* (Olivar *et al.*, 2001; Sabates *et al.*, 2008). As for larvae of
422 mesopelagic taxa, which widely dominated the LFC, show a deeper distribution, even
423 below the thermocline (Olivar *et al.*, 2010; Olivar and Sabates, 1997; Rodriguez *et al.*,
424 2006; Sabates, 2004). Only two Gonostomatidae species *Cyclothone braueri* and *C.*
425 *pygmaea* and the Myctophydae *Ceratoscopelus maderensis* reach the surface mixed
426 layer (Olivar *et al.*, 2010; Rodriguez *et al.*, 2006; Torres *et al.*, 2011). That is to say, the
427 vertical distribution of larval food would be favourable for most oceanic-mesopelagic
428 larvae and also for larvae of neritic species, which are able to perform diel vertical

migration. Also, the larvae of tuna and most neritic species, with shallow vertical distribution, would be favoured because they would not have to share the scarce trophic resources of the surface layers. The lack of correlation between larval fish abundance and mesozooplankton biomass may be explained either by the consumption of zooplankton by fish larvae or the fact that, as indicated above, our sampling may have not included the zooplankton maximum.

Neritic larvae advected offshore do not necessarily have to get lost for the adult neritic fish populations of the islands. They may return to the island shelves, either passively transported by eddies (Franco *et al.*, 2006; Lobel and Robinson, 1986) or actively swimming (Leis, 2007; Leis and Carson-Ewart, 1997; Stobutzki and Bellwood, 1997). In this case, eddies would also function as a nursery area for these larvae (Govoni *et al.*, 2010; Lobel and Robinson, 1986; Logerwell and Smith, 2001; Sabates *et al.*, 2013). It has to be indicated that neritic larvae caught in the oceanic region were advanced larvae (even juveniles), in apparently very good condition (author's personal observation). Moreover, some of these larvae, e.g. *Mullus* and Bothidae species, have a long pelagic stage (Macpherson and Raventos, 2006; Russell, 1976). These two aspects would increase the chance of survival for those larvae.

Multivariate analysis indicates that depth and, consequently, the spawning location of adult fishes were the main factors in shaping the horizontal structure of the LFC. This is consistent with that reported in previous LFC studies in our study area (Alemany *et al.*, 2006), other regions in the Mediterranean Sea (Sabates, 1990; Somarakis *et al.*, 2011) and elsewhere in the world (Auth, 2008; Muhling and Beckley, 2007; Rodriguez *et al.*, 2009). The influence of depth on larval fish distribution is clear in the case of larvae of neritic species, which most of them clustered on the very right side of the CCA biplot, but not for oceanic taxa. The clustering of most of these taxa near the centre of the

454 CCA biplot suggests that their distribution was little influenced by any of the
455 environmental variables considered in this study (ter Braak, 1986). However, in the case
456 of depth this may be an artefact caused by the narrowness of the island shelf. In fact,
457 88% of the ichthyoplankton stations were deeper than 200 m and 95% were deeper than
458 100 m. This would explain the high percentage of occurrences and the wide horizontal
459 distribution shown by many oceanic taxa. For its part, the significant correlation found
460 between larval abundances and geostrophic velocity suggests some accumulation of fish
461 larvae in anticyclonic eddy borders. This agrees with Lindo-Atichati *et al.* (2012) who,
462 in the Gulf of Mexico, found higher densities of *T. thynnus* and *Auxis* spp in the
463 boundaries of anticyclonic eddy regions.

464 The apparently low influence that mesoscale oceanographic features had on the
465 horizontal structure of the LFC in this highly dynamic region contrasts with the large
466 influence that mesoscale features have on the horizontal structure of the LFC in similar
467 regions, e.g. off the nearby Catalan coast (Olivar *et al.*, 2010; Sabates, 1990; Sabates *et*
468 *al.*, 2007) and other places around the world (Franco *et al.*, 2006; Holliday *et al.*, 2011;
469 Keane and Neira, 2008; Rodriguez *et al.*, 2004). The scenario of relatively high
470 hydrographic stability found during the cruise should explain the low influence of
471 mesoscale oceanographic features on the horizontal structure of the LFC. Also, the
472 presence of only two LFAs, a coastal and an offshore, reported for other regions with a
473 narrow continental shelf (Auth and Brodeur, 2006; Richardson and Pearcy, 1977;
474 Rodriguez *et al.*, 2009), indicates that, despite the narrowness of the shelf, most neritic
475 larvae remain in the neritic region and most oceanic larvae in the oceanic region. This
476 would agree with the above mentioned Basterretxea *et al*. (2012) simulation results that
477 suggest most neritic larvae during summer, in the Balearic Islands, remain in the neritic
478 region.

In summary, the Balearic region during early summer harbours a relatively abundant and diverse LFC dominated by larvae of oceanic mesopelagic species. Larval fish assemblages were mainly delineated by depth and consequently by the spawning location of adult fish. Thus, our hypothesis that the structure of the LFC should reflect the mesoscale oceanographic features of the region was not confirmed. The unusual, from the meteorological and hydrographical point of view, 2005 year and the scenario of higher-than usual hydrographic stability would be responsible for the relatively lack of mesoscale features and, consequently, for the lack of influence of these features on the horizontal distribution and structure of the LFC.

Acknowledgments

This work was funded by the Spanish research grant CTM2009-07944 (subprogram MAR). Authors thank to the associate editor of Deep Sea Research I, Dr Monty Priede, and three anonymous reviewers for their very useful comments and suggestions.

References

Ahlstrom, E.H., 1959. Vertical distribution of pelagic fish eggs and larvae off California and Baja California. Fishery Bulletin 161 (60), 107-146.

Alcaraz, M., 1985. Vertical distribution of zooplankton biomass during summer stratification in the Western Mediterranean. In: Gibbs, P.E. (Ed.), 19th EMBS Proceedings. Cambridge University Press, Cambridge, pp. 135-143.

Alcaraz, M., Calbet, A., Estrada, M., Marrase, C., Saiz, E., Trepat, I., 2007. Physical control of zooplankton communities in the Catalan Sea. Progress in Oceanography 74, 294-312.

Alemany, F., 1997. Ictioplancton del Mar Balear. Ph.D. Thesis, Univ. Illes Balears, Palma de Mallorca, unpublished.

Alemany, F., Deudero, S., Morales-Nin, B., Lopez-Jurado, J.L., Jansa, J., Palmer, M., Palomera, I., 2006. Influence of physical environmental factors on the composition and horizontal distribution of summer larval fish assemblages off Mallorca island (Balearic archipelago, western Mediterranean). Journal of Plankton Research 28 (5), 473-487

Alemany, F., Quintanilla, L., Velez-Belchi, P., Garcia, A., Cortes, D., Rodriguez, J.M., Fernandez de Puelles, M.L., Gonzalez-Pola, C., Lopez-Jurado, J.L., 2010.

Characterization of the spawning habitat of Atlantic bluefin tuna and related species in the Balearic Sea (western Mediterranean). Progress in Oceanography 86 (1-2), 21-38.

Auth, T.D., 2008. Distribution and community structure of ichthyoplankton from the northern and central California Current in May 2004-06. Fisheries Oceanography 17 (4), 316-331.

Auth, T.D., Brodeur, R.D., 2006. Distribution and community structure of ichthyoplankton off the coast of Oregon, USA, in 2000 and 2002. Marine Ecology Progress Series 319, 199-213.

Bakun, A., 2006. Fronts and eddies as key structures in the habitat of marine fish larvae: opportunity, adaptative response and competitive advantage. Scientia Marina 72S, 105-122.

Bakun, A., 2012. Ocean eddies, predator pits and bluefin tuna: implications of an inferred 'low risk–limited payoff' reproductive scheme of a (former) archetypical top predator. Fish and Fisheries DOI: 10.1111/faf.12002.

Basterretxea, G., Jordi, A., Catalan, I.A., Sabates, A., 2012. Model-based assessment of local-scale fish larval connectivity in a network of marine protected areas. Fisheries Oceanography 21 (4), 291-306.

Bray, J.R., Curtis, J.T., 1957. An ordination of the upland forest communities of southern Wisconsin. Ecological Monographs 27, 325-3459.

Bretherton, F.P., Davis, R.E., Fandry, C.B., 1976. A technique for objective analysis and design of oceanographic experiments applied to MODE-73. Deep Sea Research I 23 (7), 559-582.

Clarke, K.R., Ainsworth, M., 1993. A method of linking multivariate community structure to environmental variables. Marine Ecology Progress Series 92, 205-219.

Clarke, R.K., Warwick, R.M., 2001. Changes in Marine Communities: an Approach to Statistical Analysis and Interpretation, second ed. PRIMER-E, Plymouth, UK.

Estrada, M., 1996. Primary production in the northwestern Mediterranean. Scientia Marina 60 ((Supl. 2)), 55-64.

Estrada, M., Marrase, Latasa, M., Margalef, R., Delgado, M., Riera, T., 1993. Variability of deep chlorophyll maximum characteristics in the Northwestern Mediterranean. Marine Ecology Progress Series 92, 289-300.

Fernández de Puelles, M.L., Alemany, F., Jansá, J., 2007. Zooplankton time-series in the Balearic Sea (Western Mediterranean): Variability during the decade 1994-2003. Progress in Oceanography 74 (2), 329-354.

Field, J.G., Clarke, K.R., Warwick, R.M., 1982. A Practical Strategy for Analyzing Multispecies Distribution Patterns. Marine Ecology Progress Series 8 (1), 37-52.

Font, J., Isern-Fontanet, J., Salas, J.J., 2004. Tracking a big anticyclonic eddy in the Western Mediterranean. Scientia Marina 68 (3), 331-342.

Franco, B.C., Muelbert, J.H., Mata, M.M., 2006. Mesoscale physical processes and the distribution and composition of ichthyoplankton on the southern Brazilian shelf break. Fisheries Oceanography 15 (1), 37-43.

Govoni, J.J., Hare, J.A., Davenport, E.D., Chen, M.H., Marancik, K.E., 2010. Mesoscale, cyclonic eddies as larval fish habitat along the southeast United States shelf: a Lagrangian description of the zooplankton community. ICES Journal of Marine Science 67 (3), 403-411.

Holliday, D., Beckley, L.E., Olivar, M.P., 2011. Incorporation of larval fishes into a developing anti-cyclonic eddy of the Leeuwin Current off south-western Australia. Journal of Plankton Research 33 (11), 1696-1708.

Hopkins, T., 1978. Physical processes of the western Mediterranean Sea. In: Kjerfve, B. (Ed.), Estuarine Transport Processes. Univ. South Carolina Press, Columbia, pp. 269-309.

Hsieh, H.Y., Lo, W.T., Wu, L.J., Liu, D.C., 2012. Larval fish assemblages in the Taiwan Strait, western North Pacific: linking with monsoon-driven mesoscale current system. Fisheries Oceanography 21 (2-3), 125-147.

Jansa, J., Aparicio, A., Valencia, J., Amengual, B., 2004. Máximos de clorofila fitoplanctónica en la época cálida del Mar Balear. In: Pons, G.X. (Ed.), IV Jornades de Medi Ambient de les Illes Balears. Ponencies i Resums. Societat d'Historia Natural de les Balears, Palma de Mallorca, p. 232.

Jansa, J., Lopez-Jurado, J.L., Morillas, A., Amengual, B., 1998. Seasonal and mesoscale variability of biological and chemical parameters related to the hydrodynamics of the Ibiza Channel (western Mediterranean) Boletin del Instituto Espanol de Oceanografia 14 (1 y 2), 31-37.

Keane, J.P., Neira, F.J., 2008. Larval fish assemblages along the south-eastern Australian shelf: linking mesoscale non-depth-discriminate structure and water masses. Fisheries Oceanography 17 (4), 263-280.

Le Fevre, J., 1986. Aspects of the biology of frontal systems., Advances in Marine Biology.

Leis, J.M., 1982. Nearshore distributional gradients of larval fish (15 taxa) and planktonic crustaceans (6 taxa) in Hawaii. Marine Biology 72 (1), 89-97.

Leis, J.M., 2007. Behaviour as input for modelling dispersal of fish larvae: behaviour, biogeography, hydrodynamics, ontogeny, physiology and phylogeny meet hydrography. Marine Ecology-Progress Series 347, 185-193.

Leis, J.M., Carson-Ewart, B.M., 1997. In situ swimming speeds of the late pelagic larvae of some Indo-Pacific coral-reef fishes. Marine Ecology Progress Series 159, 165-174.

Leps, J., Smilauer, P., 2003. Multivariate analysis of ecological data using CANOCO. Cambridge University Press, Cambridge, UK.

Lindo-Atichati, D., Bringas, F., Goni, G., Muhling, B., Muller-Karger, F.E., Habtes, S., 2012. Varying mesoscale structures influence larval fish distribution in the northern Gulf of Mexico. Marine Ecology Progress Series 463, 245-257.

Lobel, P.S., Robinson, A.R., 1986. Transport and entrapment of fish larvae by ocean mesoscale eddies and currents in Hawaiian waters. Deep-Sea Research 33 (4), 483-500.

Lobel, P.S., Robinson, A.R., 1988. Larval fishes and zooplankton in a cyclonic eddy in Hawaiian waters. Journal of Plankton Research 10, 1209-1223.

Logerwell, E.A., Smith, P.E., 2001. Mesoscale eddies and survival of late stage Pacific sardine (*Sardinops sagax*) larvae. Fisheries Oceanography 10 (1), 13-25.

Lopez-Jurado, J., Marcos, M., Monserrat, S., 2008. Hydrographic conditions affecting two fishing grounds of Mallorca island (Western Mediterranean): during the IDEA Project (20032-2004). Journal of Marine Systems 71, 303-315.

Lopez-Jurado, J.L., Garcia-Lafuente, J., Cano, N., 1995. Hydrographic conditions of the Ibiza Channel during November 1990. March 1991 and July 1992. Oceanologica Acta 18 (2), 235-243.

Lopez-Jurado, J.L., Gonzalez-Pola, C., Velez-Belchí, P., 2005. Observation of an abrupt disruption of the long-term warming trend at the Balearic Sea, western Mediterranean Sea, in summer 2005. Geophysical Research Letters 32 (L24606), doi: 10.1029/2005GL024430.

Lovegrove, T., 1966. The determination of the dry weight of plankton and the effect of various factors on the values obtained. Some Contemporary Studies in Marine Science, 429-467.

Macpherson, E., Raventos, N., 2006. Relationship between pelagic larval duration and geographic distribution of Mediterranean littoral fishes. Marine Ecology Progress Series 327, 257265.

Millot, C., 1985. Some features of the Algerian current. Journal of Geophysical Research 90 (C4), 7169-7176.

Millot, C., 1987. Circulation in the Western Mediterranean. Oceanologica Acta 10 (2), 143-149.

Millot, C., 1999. Circulation in the Western Mediterranean Sea. Journal of Marine Systems 20 (423-442).

Moyano, M., Hernandez-Leon, S., 2011. Intra- and interannual variability in the larval fish assemblage off Gran Canaria (Canary Islands) over 2005-2007. Marine Biology 158 (2), 257-273.

Muhling, B.A., Beckley, L.E., 2007. Seasonal variation in horizontal and vertical structure of larval fish assemblages off south-western Australia, with implications for larval transport. Journal of Plankton Research 29 (11), 967-983.

Muhling, B.A., Beckley, L.E., Koslow, J.A., Pearce, A.F., 2008. Larval fish assemblages and water mass structure off the oligotrophic south-western Australian coast. Fisheries Oceanography 17 (1), 16-31.

Mullaney, T.J., Miskiewicz, A.G., Baird, M.E., Burns, P.T.P., Suthers, I.M., 2011. Entrainment of larval fish assemblages from the inner shelf into the East Australian Current and into the western Tasman Front. Fisheries Oceanography 20 (5), 434-447.

Olivar, M.P., Emelianov, M., Villate, F., Uriarte, I., Maynou, F., ALvarez, I., Morote, E., 2010. The role of oceanographic conditions and plankton availability in larval fish assemblages off the Catalan coast (NW Mediterranean). Fisheries Oceanography 19 (3), 209-229.

Olivar, M.P., Sabates, A., 1997. Vertical distribution of fish larvae in the north-west Mediterranean Sea in spring. Marine Biology 129 (2), 289-300.

Olivar, M.P., Salat, J., Palomera, I., 2001. Comparative study of the spatial distribution patterns of the early stages of anchovy and pilchard in the NW Mediterranean Sea. Marine Ecology Progress Series 217, 111-120.

Pedder, M.A., 1993. Interpolation and filtering of spatial observations using successive corrections and Gaussian filters. Monthly Weather Review 121, 2889-2902.

P , J., Gomis, D., 1996. Quasi-synoptic mesoscale variability in the balearic sea. Deep Sea Research Part I 41, 897–914.

Pinot, J.M., Lopez-Jurado, J.L., Riera, M., 2002. The CANALES experiment (1996–1998). Interannual, seasonal and mesoscale variability of the circulation in the Balearic Channels. Progress in Oceanography 55, 335-370.

Richardson, S.L., Pearcy, W.G., 1977. Coastal and oceanic fish larvae in an area of upwelling off Yaquina Bay, Oregon. Fishery Bulletin 75 (1).

Rodriguez, J.M., 1990. Contribución al conocimiento del ictioplancton del Mar de Alborán. Boletin del Instituto Español de Oceanografia 6 (1), 1-20.

Rodriguez, J.M., Barton, E.D., Hernandez-Leon, S., Aristegui, J., 2004. The influence of mesoscale physical processes on the larval fish community in the Canaries-CTZ, in summer. Progress in Oceanography 62, 171-188.

Rodriguez, J.M., Gonzalez-Nuevo, G., Gonzalez-Pola, C., Cabal, J., 2009. The ichthyoplankton assemblages and the environmental variables off the NW and N Iberian Peninsula coasts, in early spring. Continental Shelf Research 29, 1145-1156.

Rodriguez, J.M., Hernandez-Leon, S., Barton, E.D., 2006. Vertical distribution of fish larvae in the Canaries-African coastal transition zone in summer. Marine Biology 149, 885-897.

Russell, F.S., 1976. The eggs and planktonic stages of British marine fishes. Academic Press, London.

Sabates, A., 1990. Distribution pattern of larval fish populations in the northwestern Mediterranean. Marine Ecology Progress Series 59 (1-2), 75-82.

Sabates, A., 2004. Diel vertical distribution of fish larvae during the winter-mixing period in the northwestern Mediterranean. ICES Journal of Marine Science 61, 1243-1252.

Sabates, A., Olivar, M.P., 1996. Variation of larval fish distributions associated with variability in the location of a shelf-slope front. Marine Ecology Progress Series 135 (1-3), 11-20.

Sabates, a., Olivar, M.P., Salat, J., Palomera, I., Alemany, F., 2007. Physical and biological processes controlling the distribution of fish larvae in the NW Mediterranean. Progress in Oceanography 74, 355-376.

Sabates, A., Salat, J., R., V., Emelianov, M., 2013. Role of mesoscale eddies in shaping the spatial distribution of the coexisting *Engraulis encrasicolus* and *Sardinella aurita* larvae in the northwestern Mediterranean. Journal of Marine Systems 111–112, 108-119.

Sabates, A., Salat, J., Raya, V., Emelianov, M., Segura-Noguera, M., 2009. Spawning environmental conditions of *Sardinella aurita* at the northern limit of its distribution range, the western Mediterranean. Marine Ecology Progress Series 385, 227-236.

Sabates, A., Zaragoza, N., Grau, C., Salat, J., 2008. Vertical distribution of early developmental stages in two coexisting clupeoid species, *Sardinella aurita* and *Engraulis encrasicolus*. Marine Ecology Progress Series 364, 169-180.

Saiz, E., Calbet, A., Atienza, D., Alcaraz, M., 2007. Feeding and production of zooplankton in the Catalan Sea (NW Mediterranean) Progress in Oceanography 74 (2-3), 313-328.

Salat, J., 1995. The interaction between the Catalan and Balearic currents in the southern Catalan sea. Oceanologica Acta 18, 227-234.

Somarakis, S., Drakopoulos, P., Filippou, V., 2002. Distribution and abundance of larval fish in the northern Aegean Sea -eastern Mediterranean- in relation to early summer oceanographic conditions. Journal of Plankton Research 24 (4), 339-358.

Somarakis, S., Isari, S., Machias, A., 2011. Larval fish assemblages in coastal waters of central Greece: reflections of topographic and oceanographic heterogeneity. Scientia Marina 75 (3), 605-618.

Sournia, A., 1994. Pelagic biogeography and fronts. Progress in Oceanography 34, 109-120.

694 Stobutzki, I.C., Bellwood, D.R., 1997. Sustained swimming abilities of the late pelagic
695 stages of coral reef fishes. Marine Ecology Progress Series 149, 35.41.
696 ter Braak, C.J.F., Smilauer, P., 2002. CANOCO reference manual and CanoDraw for
697 Windows user's guide: software for canonical community ordination (version 4.5).
698 Microcomputer Power, Ithaca, NY.
699 ter Braak, C.J.F., Verdonschot, P.F.M., 1995. Canonical correspondence analysis and
700 related multivariate methods in aquatic ecology. Aquatic Sciences 57 (3), 255-289.
701 ter Braak, J.F., 1986. Canonical correspondence analysis: A new eigenvector technique
702 for multivariate direct gradient analysis. Ecology 67 (5), 1167-1179.
703 Tintore, J., Gomis, D., Alonso, S., Parrilla, G., 1991. Mesoscale dynamics and vertical
704 motion in the Alboran Sea. Journal of Physical Oceanography 21, 811-823.
705 Tintore, J., La Violette, P.E., Blade, I., Cruzado, A., 1988. A study of an intense density
706 front in the eastern Alboran Sea: The Almeria-Oran Front. Journal of Physical
707 Oceanography 18 (10), 1384-1397.
708 Torres, A.P., Reglero, P., Balbin, R., Urtizberea, A., Alemany, F., 2011. Coexistence of
709 larvae of tuna species and other fish in the surface mixed layer in the NW
710 Mediterranean. Journal of Plankton Research 33 (12), 1793-1812.
711 Zarrad, R., Alemany, F., Rodriguez, J.M., Jarboui, O., Lopez-Jurado, J.L., Balbin, R.,
712 2013. Influence of summer conditions on the larval fish assemblage in the eastern coast
713 of Tunisia (Ionian Sea, Southern Mediterranean). Journal of Sea Research 76, 114-125.
714

715 Figure legends

716 Fig. 1. Map of the western Mediterranean Sea showing the study area (shadow zone)
717 and the main hydrographic features of the region

718 Fig. 2. Horizontal distribution of (a) sea surface salinity (salinity at 10 m depth) and (b)
719 dynamic height (cm) at 10 decibars (db) relative to 600 db and derived geostrophic
720 currents at 10 m depth

721 Fig. 3. Average temperature (T) and fluorescence (F) profiles

722 Fig. 4. Horizontal distribution of depth-integrated (5-200 m) fluorescence and
723 mesozooplankton biomass

724 Fig. 5. Horizontal distribution of fish larvae

725 Fig. 6. Horizontal distribution of taxon richness and diversity of fish larvae

726 Fig. 7. (a) Hierarchical clustering, (b) non-metric multidimensional scaling (MDS)
727 ordination and (c) geographical location of the larval fish assemblages based on the
728 Bray Curtis similarity matrix of Log_e (x+1) transformed abundance of fish larvae

729 Fig. 8. (a) Hierarchical clustering and (b) non-metric multidimensional scaling (MDS)
730 ordination of the species assemblages based on the Bray Curtis similarity matrix of Log_e
731 (x+1) transformed abundance of fish larvae

732 Fig. 9. CCA biplot for environmental variables (arrows) and larval fish taxa (triangles).
733 Environmental variables were depth (D), sea surface salinity (SSS), dynamic height
734 (DH), geostrophic velocity (GV), depth-integrated fluorescence (IF) and
735 mesozooplankton biomass (MB). See Table1 for larval fish species codes

736 Fig. 10. Geographical distribution of axes 1 and 2 CCA sample scores

Table I

Click here to download Table: Lista taxonmica sin autor_4.docx

Table I. Alphabetical list of larval fish families collected in the Balearic Sea, in July 2005, taxa code (Code), their relative abundance (RA, %) and their percentage of occurrence (%O)

Family and species	Code	RA	%O
Apogonidae			
Apogon (Apogon) imberbis		0.031	3.3
Argentinidae			
Glossanodon leioglossus		0.002	0.5
Blenniidae			
Parablennius pilicornis		0.002	0.5
Unidentified sp		0.020	
Bramidae			
Brama brama		0.004	1.1
Bothidae			
Arnoglossus imperialis		0.002	0.5
Arnoglossus laterna		0.009	1.6
Arnoglossus rueppelli		0.007	1.6
Arnoglossus thori	*At*	0.062	9.8
Bothus podas		0.019	4.9
Arnoglossus spp	*A*spp	0.084	7.1
Callionymidae			
Callionymus spp	*C*spp	0.048	9.3
Caproidae			
Capros aper		0.011	3.3
Carangidae			
Trachinotus ovatus		0.002	0.5
Trachurus mediterraneus	*Tm*	0.434	20.2
Trachurus spp	*T*spp	0.871	13.7
Seriola dumerili		0.035	4.9
Carapidae			
Carapus acus		0.002	0.5
Cepolidae			
Cepola rubescens	*Cr*	0.299	15.8
Chlorophthalmidae			
Chlorophthalmus agassizii		0.002	0.5
Clupeidae			
Sardinella aurita	*Sa*	1.638	25.7
Centracanthidae			
Spicara flexuosa		0.002	0.5
Spicara smaris	*Ss*	0.420	8.7
Spicara spp		0.009	0.5
Centriscidae			
Macroramphosus scolopax		0.002	0.5
Congridae			
Ariosoma balearicum		0.002	0.5
Coryphaenidae			
Coryphaena hippurus		0.004	1.1
Dactylopteridae			
Dactylopterus volitans		0.007	1.6
Engraulidae			
Engraulis encrasicolus	*Ee*	1.365	33.9

Table I. Continued

Family and species	Code	RA	%O
Evermannellidae			
Evermannella balbo		0.030	6.0
Exocoetidae			
Hirundichthys sp		0.002	0.5
Gobiidae			
Aphia minuta	*Am*	0.100	6.0
Crystallogobius linearis		0.058	1.1
Gobius niger	*Gn*	0.110	7.7
Gobius paganellus		0.002	0.5
Lebetus guilleti	*Lg*	0.048	7.1
Pomatoschistus marmoratus		0.009	0.5
Pomatoschistus minutus		0.002	0.5
Pseudaphya ferreri	*Pf*	0.963	14.2
Gobiidae sp 1		0.032	0.5
Gobiidae sp 2		0.002	0.5
Gobiidae sp 3		0.004	1.1
Unidentified spp		0.036	4.9
Gonostomatidae			
Cyclothone braueri	*Cb*	24.615	98.9
Cyclothone pygmaea	*Cp*	7.584	91.8
Unidentified spp		0.005	1.6
Labridae			
Coris julis	*Cl*	0.582	31.1
Thalassoma pavo		0.018	2.7
Symphodus sp 1		0.007	1.1
Symphodus sp 2		0.007	1.6
Symphodus sp 3		0.021	3.3
Symphodus spp		0.002	0.5
Xyrichthys novacula		0.014	2.2
Lophotidae			
Lophotus lacepedei		0.002	0.5
Merlucciidae			
Merluccius merluccius		0.006	1.6
Mugilidae			
Mugil spp		0.011	2.7
Mullidae			
Mullus barbatus	*Mb*	0.040	6.0
Mullus surmuletus		0.005	1.6
Unidentified spp		0.035	4.4
Muraenidae			
Unidentified spp		0.002	0.5
Myctophidae			
Benthosema glaciale	*Bg*	1.936	60.7
Ceratoscopelus maderensis	*Cm*	14.297	97.8
Diaphus holti		0.038	9.8
Diaphus spp		0.003	1.1
Electrona rissoi		0.004	0.5
Hygophum spp	*H*spp	25.060	95.1
Lampanyctus crocodilus	*Lc*	4.216	89.1
Lampanyctus pusillus	*Lp*	2.219	84.7

Table I. Continued

Family and species	Code	RA	%O
Lampanyctus spp		0.017	1.6
Lobianchiia dofleini	*Ld*	0.124	21.9
Lobiancha gemellarii		0.007	1.6
Notoscopelus (*Notoscopelus*) *kroeyerii*		0.023	6.6
Notoscopelus (*Pareiophus*) *bolini*		0.027	4.9
Notoscopelus spp		0.017	3.3
Myctophum punctatum	*Mp*	0.180	18.6
Symbolophorus veranyi	*Sv*	0.711	53.6
Unidentified spp		0.150	14.8
Nomeidae			
Cubiceps gracilis		0.002	0.5
Ophidiidae			
Ophidion barbatum		0.002	0.5
Parophidion vassali		0.025	4.4
Ophididae			
Unidentified spp	Ophid	0.044	7.1
Ophichthidae			
Dalophis imberbis		0.006	1.6
Paralepididae			
Lestidiops jayakari	*Lj*	0.470	55.8
Lestidiops sphyrenoides		0.036	7.1
Notolepis rissoi	*Nr*	0.221	16.9
Paralepis coregonoides	*Pc*	0.598	36.1
Unidentified spp		0.215	22.4
Phosichthyidae			
Ichthyococcus ovatus		0.007	1.6
Vinciguerria attenuata	*Va*	1.364	74.9
Pleuronectidae			
Unidentified spp		0.002	0.5
Pomacentridae			
Chromis chromis	*Cc*	0.719	37.2
Scombridae			
Auxis rochei	*Ar*	2.251	44.8
Euthynnus alletteratus	*Ea*	0.064	5.5
Katsuwonus pelamis		0.002	0.5
Scomber japonicus		0.002	0.5
Thunnus alalunga	*Ta*	1.070	61.7
Thunnus thynnus	*Tt*	0.276	18.6
Unidentified spp		0.010	0.5
Scophthalmidae			
Lepidorhombus boscii		0.002	0.5
Scorpaenidae			

Table I. Continued

Family and species	Code	RA	%O
Helicolenus dactylopterus dactylopterus		0.002	0.5
Scorpaena notata		0.005	1.6
Scorpaena porcus		0.008	2.2
Scorpaena spp		0.014	3.3
Serranidae			
Anthias anthias		0.009	2.2
Epinephelus sp		0.002	0.5
Serranus cabrilla	*Sc*	0.411	22.4
Serranus hepatus	*Sh*	0.370	16.4
Sparidae			
Diplodus annularis		0.006	1.6
Diplodus spp		0.022	3.8
Oblada melanura		0.002	0.5
Pagrus pagrus	Pp	0.128	7.1
Unidentified spp		0.018	1.6
Sternoptychidae			
Maurolicus muelleri		0.011	2.2
Stomiidae			
Borostomias antarcticus		0.004	0.5
Chauliodus sloani		0.002	0.5
Stomias boa	*Sb*	0.215	35.0
Stomiidae			
Unidentified spp		0.002	0.5
Syngnathidae			
Nerophis ophidon		0.002	0.5
Synodontidae			
Synodus saurus		0.008	2.2
Trachinidae			
Trachinus draco	*Td*	0.209	15.8
Trachinus spp		0.005	1.6
Triglidae			
Eutrigla gurnardus		0.002	0.5
Lepidotrigla cavillone		0.032	3.8
Trigloporus lastoviza		0.002	0.5
Unidentified spp		0.008	2.2
Trichiuridae			
Trichiurus lepturus		0.026	3.3
Uranoscopidae			
Uranoscopus scaber		0.002	0.5
Xiphiidae			
Xiphias gladius		0.015	4.4
Unidentified larvae		2.089	

fig. 1.tif

Click here to download high resolution image

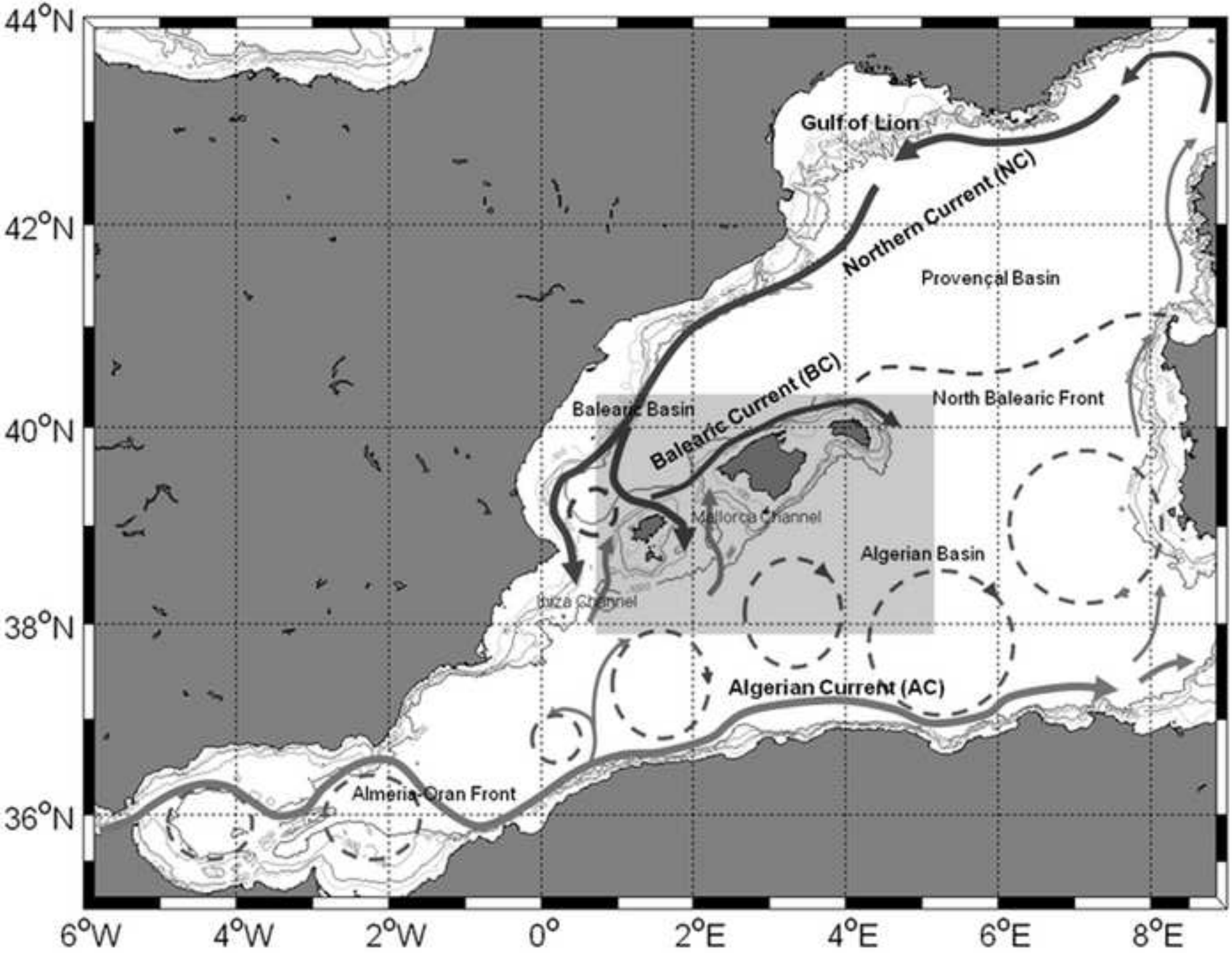

fig. 2.tif
Click here to download high resolution image

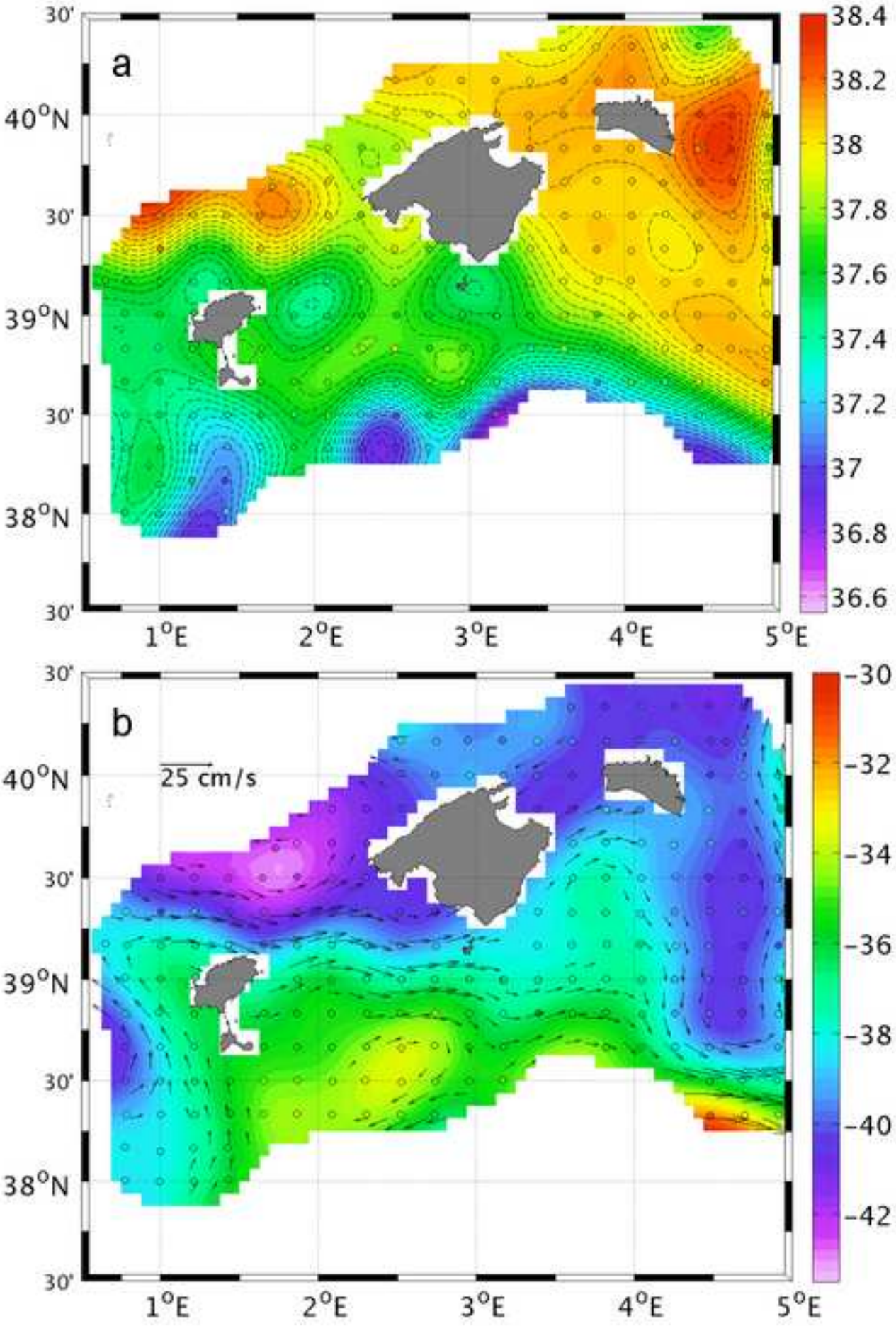

fig. 3.tif
Click here to download high resolution image

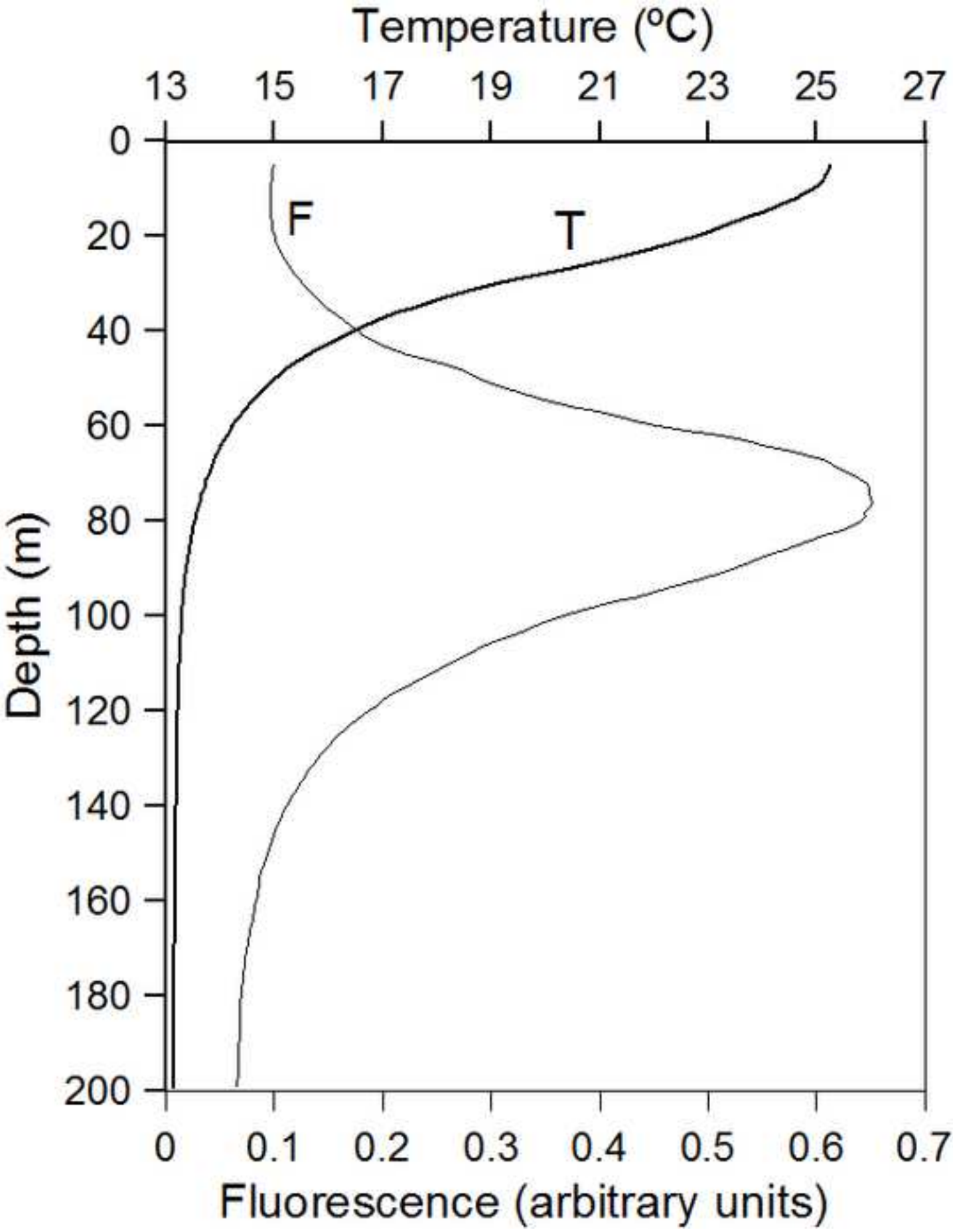

fig. 4.tif
Click here to download high resolution image

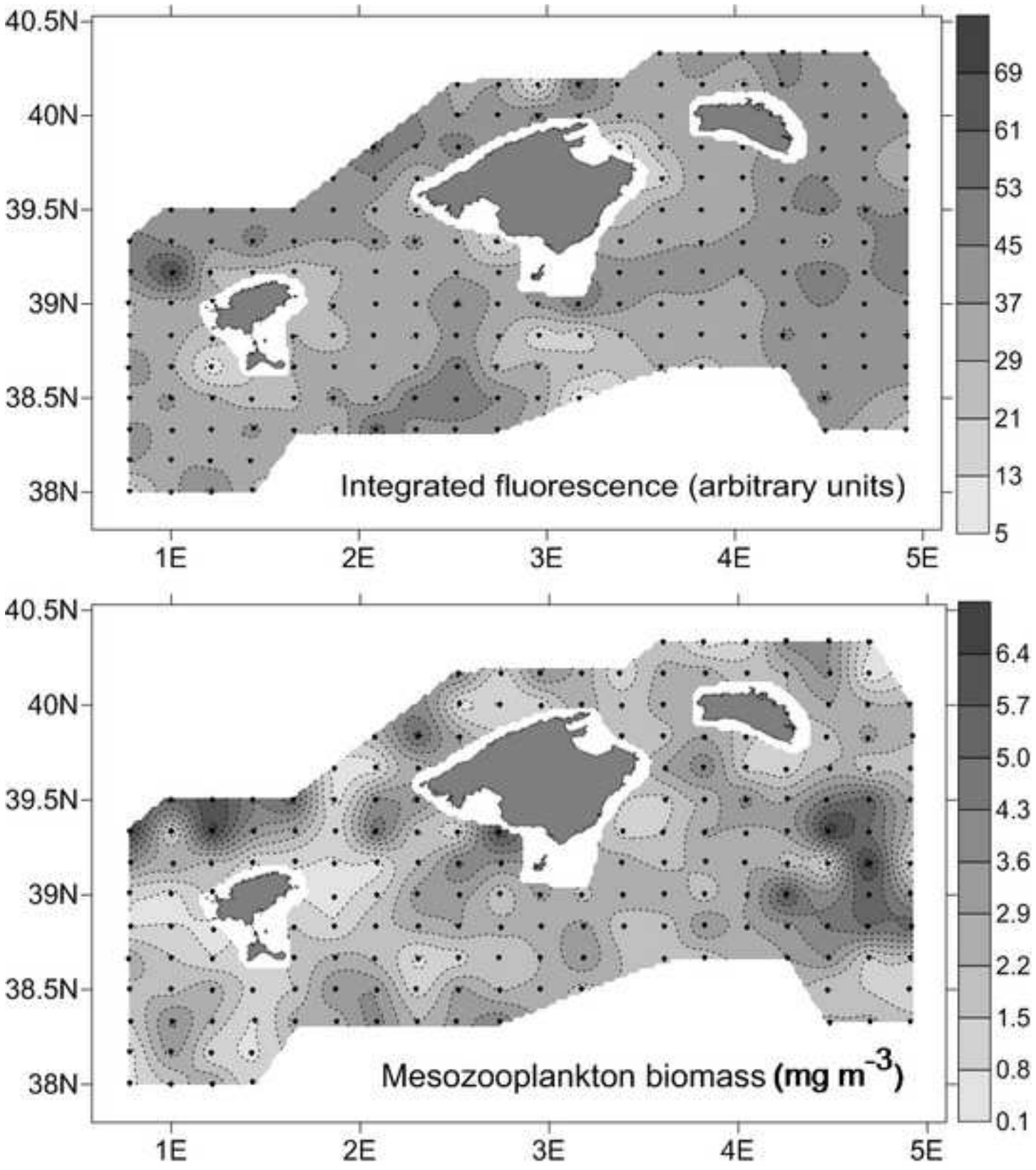

fig. 5.tif
Click here to download high resolution image

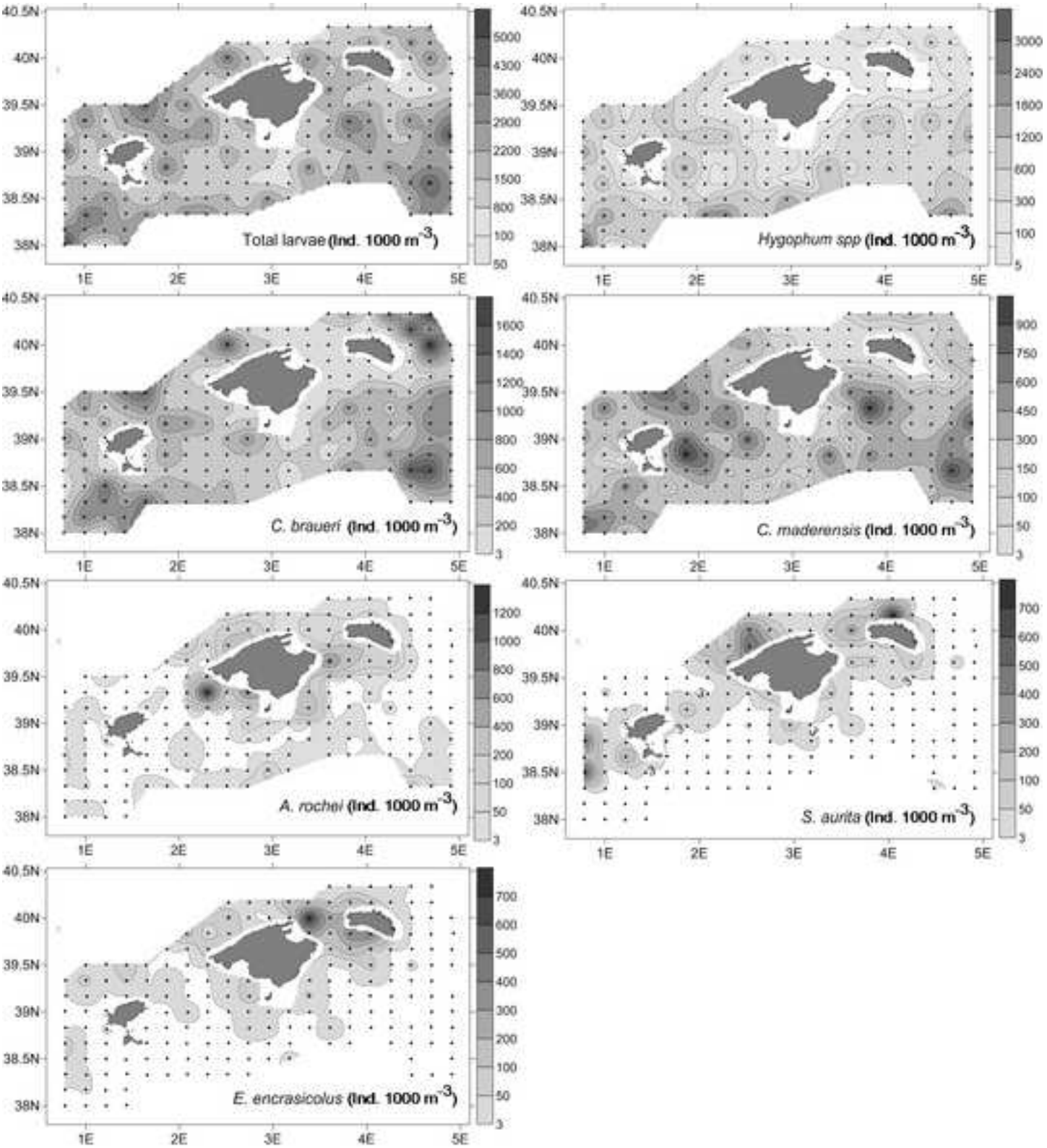

fig. 6.tif
Click here to download high resolution image

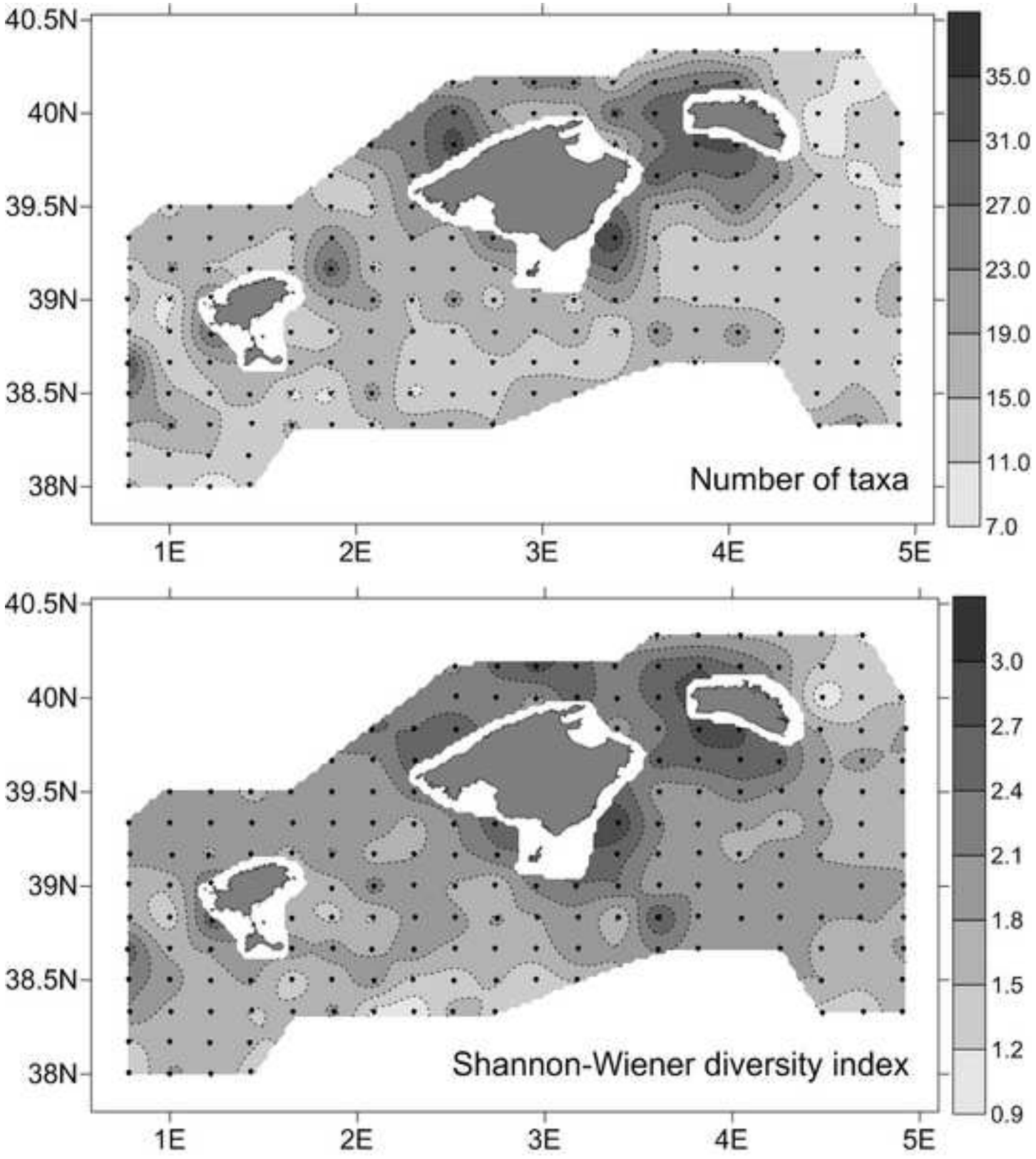

fig. 7.tif
Click here to download high resolution image

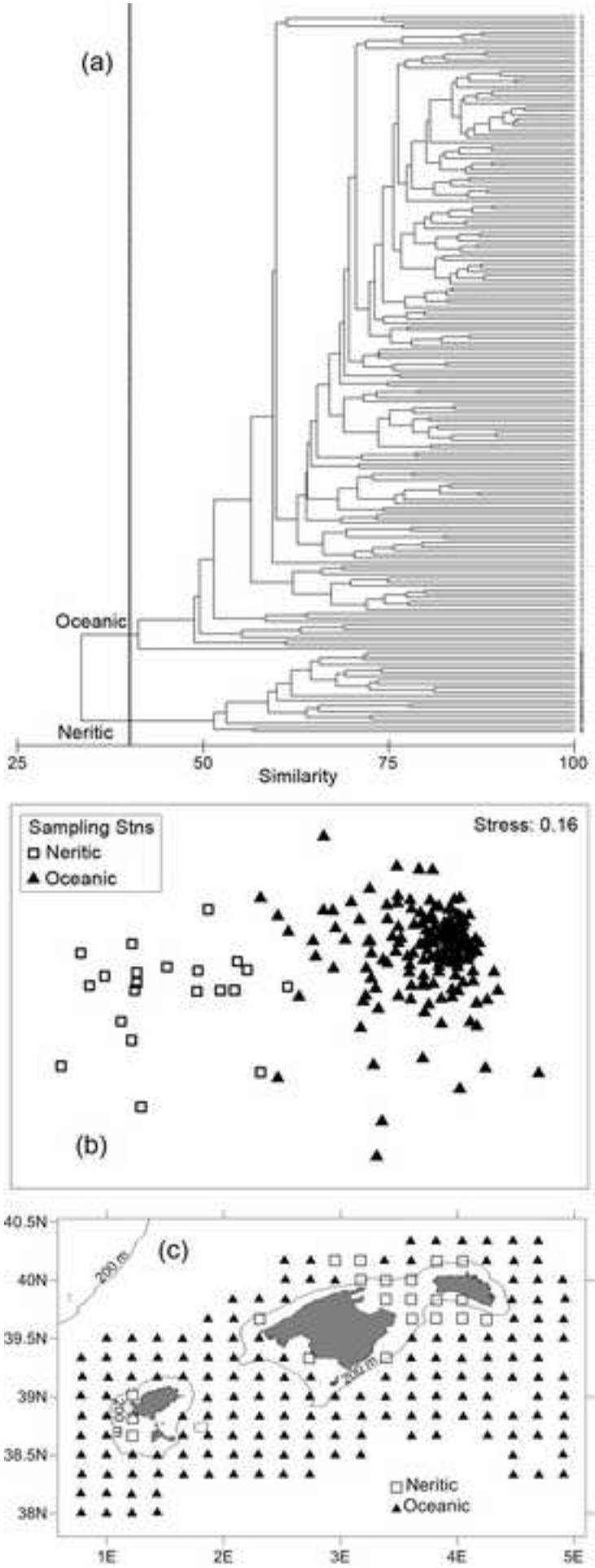

fig. 8.tif
Click here to download high resolution image

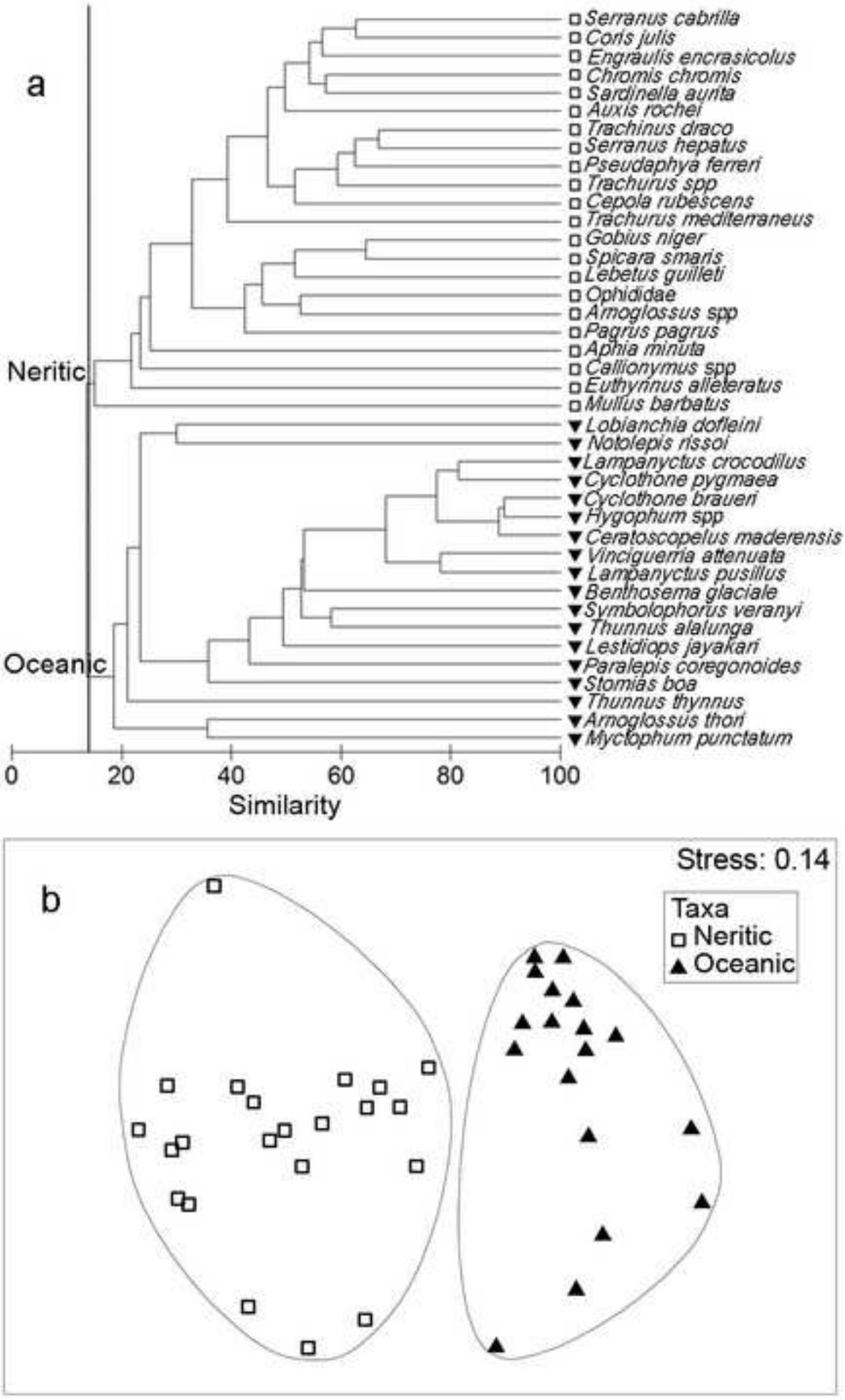

fig. 9.tif
Click here to download high resolution image

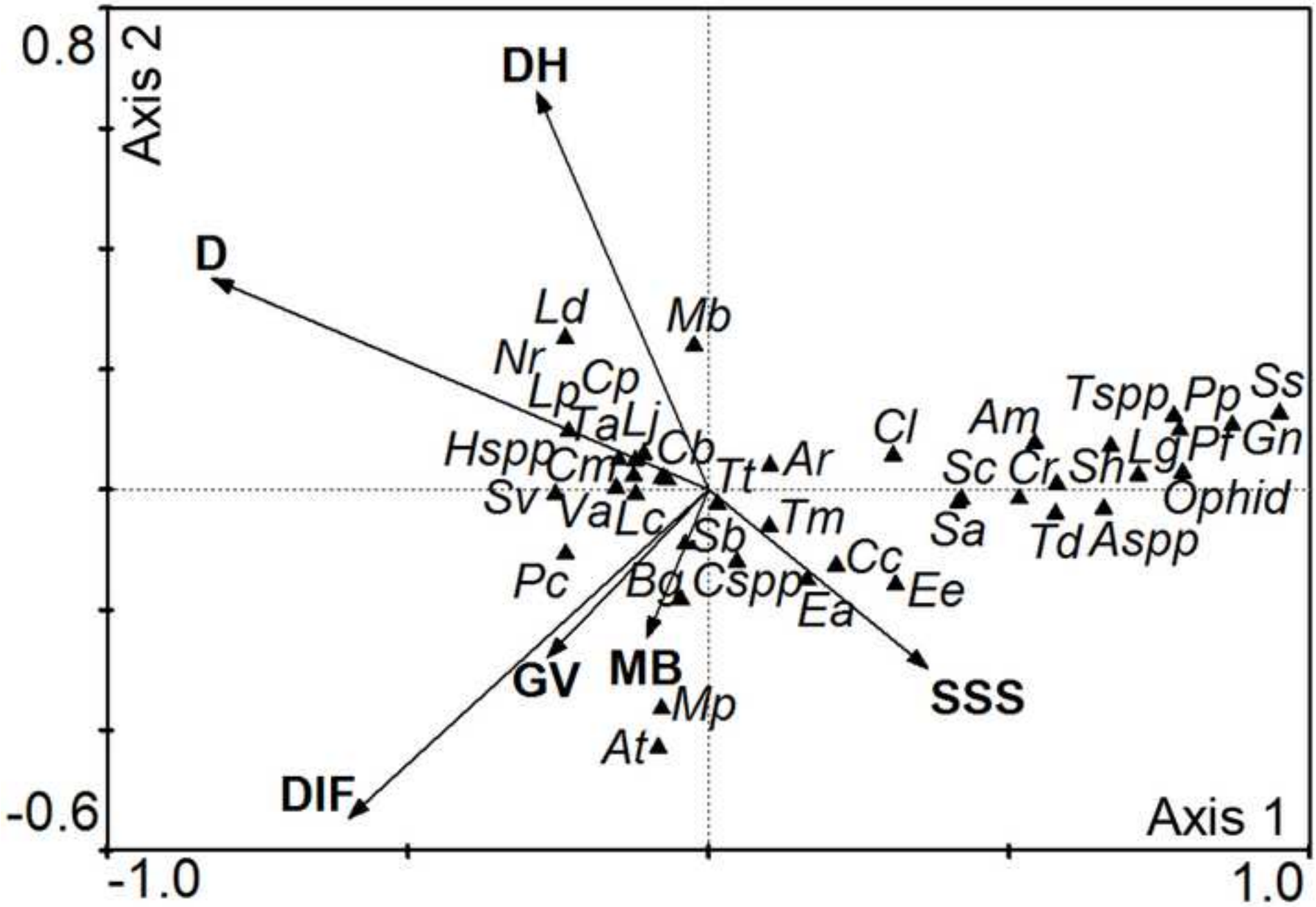
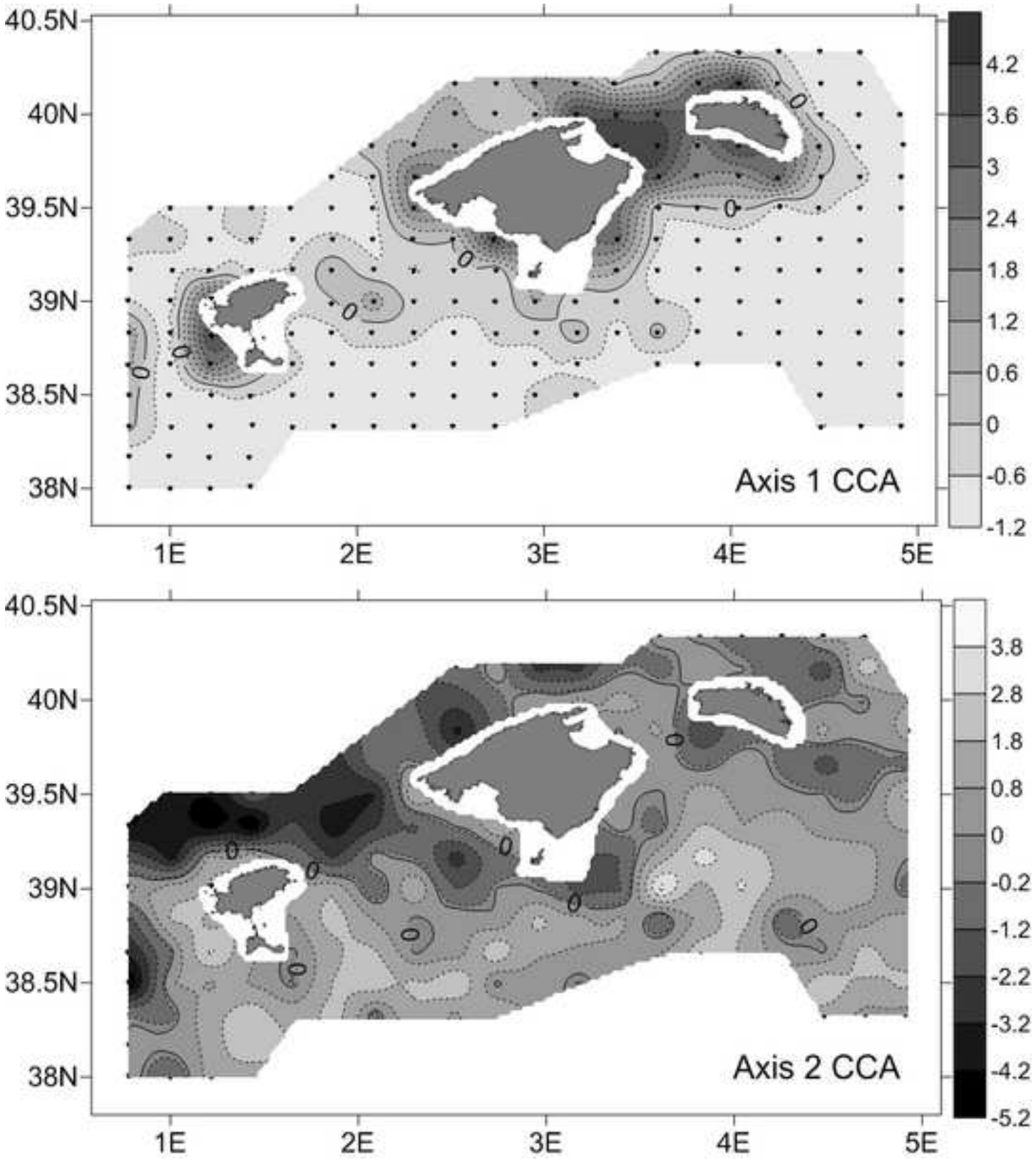
fig. 10.tif
Click here to download high resolution image